Journal of Materials Chemistry A

RSC Publishing

PAPER

View Article Online
View Journal | View Issue

Published on 07 May 2013. Downloaded by National Chiao Tung University on 28/04/2014 01:59:56.

Cite this: J. Mater. Chem. A, 2013, 1, 7767

Solution-processed benzotrithiophene-based donor molecules for efficient bulk heterojunction solar cells†

Dhananjaya Patra,[a] Chao-Cheng Chiang,[a] Wei-An Chen,[b] Kung-Hwa Wei,[c] Meng-Chyi Wu[b] and Chih-Wei Chu*[ad]

Received 18th April 2013
Accepted 7th May 2013

DOI: 10.1039/c3ta11544e

www.rsc.org/MaterialsA

In this study we used convergent syntheses to prepare two novel acceptor–donor–acceptor (A–D–A) small molecules (BT4OT, BT6OT), each containing an electron-rich benzotrithiophene (BT) unit as the core, flanked by octylthiophene units, and end-capped with electron-deficient cyanoacetate units. The number of octylthiophene units affected the optical, electrochemical, morphological, and photovoltaic properties of BT4OT and BT6OT. Moreover, BT4OT and BT6OT possess low-energy highest occupied molecular orbitals (HOMOs), providing them with good air stability and their bulk heterojunction (BHJ) photovoltaic devices with high open-circuit voltages (V_{oc}). A solar cell device containing BT6OT and [6,6]-phenyl-C_{71}-butyric acid methyl ester ($PC_{71}BM$) in a 1 : 0.75 ratio (w/w) exhibited a power conversion efficiency (PCE) of 3.61% with a short-circuit current density (J_{sc}) of 7.39 mA cm^{-2}, a value of V_{oc} of 0.88 V, and a fill factor (FF) of 56.9%. After adding 0.25 vol% of 1-chloronaphthalene (CN) as a processing additive during the formation of the blend film of BT6OT:$PC_{71}BM$ (1 : 0.75, w/w), the PCE increased significantly to 5.05% with values of J_{sc} of 9.94 mA cm^{-2}, V_{oc} of 0.86 V, and FF of 59.1% as a result of suppressed nanophase molecular aggregation.

Introduction

Harvesting solar energy through the use of solution-processable organic solar cells (OSCs) appears to be an effective strategy for controlling global energy issues. During the last decade, OSCs based on polymers have gained much attention because of their low cost, flexibility, light weight, and solution processability over large areas.[1–4] The power conversion efficiencies (PCEs) of polymer solar cells (PSCs) have increased significantly to over 8% as a result of recent developments of a variety of novel electron-donating polymers and device architectures.[5,6] Although the PCEs of small-molecule organic solar cells (SMOSCs) are much lower than those of PSCs, a few encouraging PCEs of greater than 6% have been reported recently, suggesting that SMOSCs might become promising alternatives to PSCs,[7–9] particularly because of their relatively simple purification, controlled molecular weight distributions, high open-circuit voltages (V_{oc}) and charge carrier mobilities, high purity, and reproducible solution processing.[10–12] Nevertheless, several critical issues will need to be addressed if SMOSCs are to find wider applicability, including improvements in their film quality, fill factors (FFs), and morphologies, thereby resulting in greater PCEs. For this purpose, innovations in the design of novel molecules are both urgent and challenging.

Planar electron-donating molecules containing alternating repeating units of electron donors (D) and electron acceptors (A) have been used recently in devices exhibiting promising efficiencies.[10,11] Furthermore, such D–A architectures can lower the material band gap and extend the absorption band toward longer wavelength, while simultaneously allowing effective manipulation of the energy levels of the highest occupied molecular orbital (HOMO) and lowest unoccupied molecular orbital (LUMO).[8,12] The planar D–A solution-processed OSC materials that have been reported previously have included dithienosilole,[13] benzodithiophene,[14] triphenylamine,[15] diketopyrrolopyrrole,[16] rhodanine,[17] and cyanoacetate[18–20] units as their electron-push and electron-pull moieties. Some A–D–A molecules reported by Chen and coworkers, featuring end-capped cyanoacetate acceptors, have been used in devices exhibiting promising PCEs.[18–20] Recent landmark PCEs of up to 7.4% have been achieved from a planar A–D–A molecule comprising a central donor benzodithiophene unit end-capped with rhodanine acceptors.[20] Benzotrithiophene (BT), an electron-donating candidate that is more planar and more sulfur-rich than benzodithiophene, has been copolymerized recently and with various accepting units to achieve devices with PCEs of up to 5.6%.[21,23] BT contains two free α-positions; its third fused

[a]Research Center for Applied Sciences, Academia Sinica, Taipei, Taiwan, ROC. E-mail: gchu@gate.sinica.edu.tw

[b]Institute of Electronic Engineering, National Tsing Hua University, Hsinchu, Taiwan, ROC

[c]Department of Materials Science and Engineering, National Chiao-Tung University, Hsinchu, Taiwan, ROC

[d]Department of Photonics, National Chiao-Tung University, Hsinchu, Taiwan, ROC

† Electronic supplementary information (ESI) available. See DOI: 10.1039/c3ta11544e

Published on 07 May 2013. Downloaded by National Chiao Tung University on 28/04/2014 01:59:56.

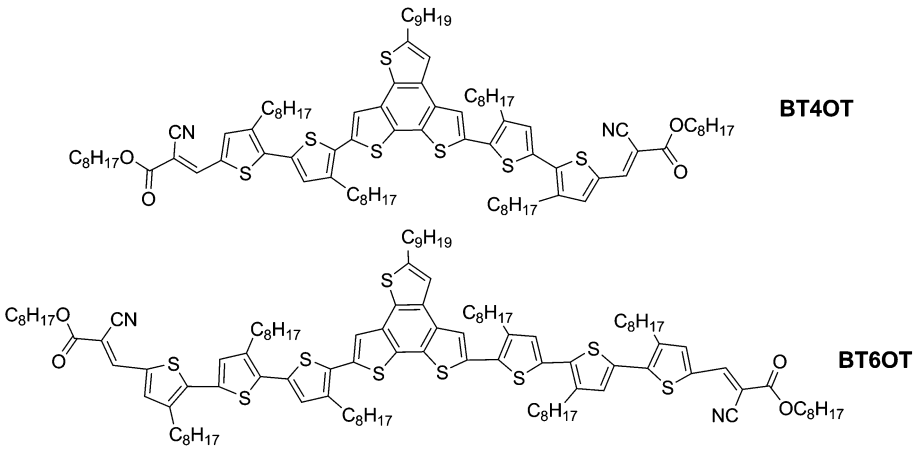

Fig. 1 Chemical structures of the small molecules BT4OT and BT6OT.

thiophene bearing a solubilizing side chain can extend the electron-donating capacity of the conjugated moiety.[24] The BT core enhances the degrees of intermolecular π–π stacking, charge transport, and mobility.[21–25] To the best of our knowledge, there have been no previous reports on BT-based solution-processed SMOSCs.

In this paper we report the synthesis and characterization of two new planar electron-donating molecules, BT4OT and BT6OT, each featuring BT as the donor unit, alkyl cyanoacetates as electron acceptor units, and octylthiophene as the bridge between them (Fig. 1). BT4OT and BT6OT differ in terms of their number of alkyl thiophene units, which affected their photophysical, electrochemical, and photovoltaic properties. We prepared the first BT-based SMOSC to exhibit excellent photovoltaic performance including a PCE of 5.05% when we used BT6OT as the electron donor, [6,6]-phenyl-C_{71}-butyric acid methyl ester ($PC_{71}BM$) as the electron acceptor, and 0.25% of 1-chloronaphthalene (CN) as the processing additive.

Experimental

Materials

All chemicals and solvents were purchased in reagent grade from Aldrich, ACROS, Fluka, or Lancaster, except $Pd(PPh_3)_4$, which was obtained from Strem Chemical. Tetrahydrofuran (THF), toluene, and diethyl ether were distilled over Na/benzophenone; all reagents were used as received.

Measurements and characterization

^1H and ^{13}C NMR spectra were recorded using a Varian Unity 300 MHz spectrometer and $CDCl_3$; chemical shifts are reported as δ values (ppm) relative to an internal tetramethylsilane (TMS) standard. Elemental analyses, determined using a HERAEUS CHN-OS RAPID elemental analyzer, and mass spectra, determined using matrix-assisted laser desorption ionization time-of-flight mass spectrometry (MALDI-TOF MS; Applied Biosystems, DE-PRO, Texas, USA), were performed in the Academia Sinica mass spectrometry laboratory. UV-Vis absorption spectra were recorded using an HP G1103A apparatus from dilute solutions in $CHCl_3$ or from solid films that had been spin-coated onto a glass substrate from $CHCl_3$ solutions (10 mg mL^{-1}). Cyclic voltammetry (CV) was performed in 0.1 M tetrabutylammonium hexafluorophosphate ($TBAPF_6$) in MeCN at room temperature using a BAS 100 electrochemical analyzer with a standard three-electrode electrochemical cell operated at a scanning rate of 100 mV s^{-1}. During the CV measurements, the solutions were purged with N_2 for 30 s. In each case, a C working electrode was coated with a thin layer of copolymers, a Pt wire was used as the counter electrode, and a Ag wire was used as the quasi-reference electrode; a Ag/AgCl (3 M KCl) electrode served as the reference electrode for all potentials quoted herein. The redox couple of ferrocene/ferrocenium ion (Fc/Fc^+) was used as an external standard. The corresponding energy levels of the highest occupied molecular orbital (HOMO) and lowest unoccupied molecular orbital (LUMO) were calculated from the experimental values of $E_{ox/onset}$ and $E_{red/onset}$ for the solid films of BT4OT and BT6OT, which were formed by drop-casting films at a similar thickness from THF solutions (*ca.* 5 mg mL^{-1}). The onset potentials were determined from the intersections of two tangents drawn at the rising currents and background currents of the CV measurements. Atomic force microscopy (AFM) images of the thin films (on glass substrates) were obtained using a Digital Instruments NS 3a controller and a D3100 stage.

Fabrication of organic solar cells (OSCs)

BHJ solar cells were prepared on a commercially available ITO-coated glass substrate in a sandwiched structure of ITO/PEDOT:PSS (40 nm)/(small molecule):PCBM (*ca.* 190 nm)/Ca (50 nm)/Al (90 nm). Prior to device fabrication, ITO-coated glass substrates (1.5 × 1.5 cm^2) were ultrasonically cleaned sequentially in detergent, deionized water, acetone, and isopropyl alcohol. After routine solvent cleaning, the ITO substrates were treated with UV ozone for 15 min and then spin-coated with the PEDOT:PSS layer (*ca.* 30 nm) at 4000 rpm. The active layer solution, BT4OT:PC61BM or BT4OT:$PC_{61}BM$ (8 mg mL^{-1} for donor materials in $CHCl_3$), was then cast upon the modified ITO substrate, after filtering through a 0.45 mm

 This journal is © The Royal Society of Chemistry 2013

Published on 07 May 2013. Downloaded by National Chiao Tung University on 28/04/2014 01:59:56.

polytetrafluoroethylene (PTFE) filter with a spin rate of 7000 rpm, for 1 min; BT6OT was also blended with $PC_{71}BM$ (8 mg mL^{-1} in $CHCl_3$) at various weight ratios in the presence of various volumes (vol%) of CN. Finally, layers of Ca (50 nm) and Al (90 nm) were thermally evaporated through a shadow mask at a pressure below 6×10^{-6} torr. All PSC devices were prepared and measured under ambient conditions; the active area of each device was 0.15 cm^2. The active layer thickness was measured using an AlphaStep profilometer (Veeo, Dektak 150). Solar cell testing was performed inside a glove box under simulated AM 1.5G irradiation (100 mW cm^{-2}) using a Xe lamp-based solar simulator (Thermal Oriel 1000 W). The EQE action spectrum was obtained under short-circuit conditions. The light source was a 450 W Xe lamp (Oriel Instrument, model 6266) equipped with a water-based IR filter (Oriel Instrument, model 6123NS). The light output from the monochromator (Oriel Instrument, model 74100) was focused onto the PV devices.

Fabrication of hole- and electron-only devices

Hole- and electron-only devices incorporating blend films of BT6OT and $PC_{71}BM$ [1 : 0.75 (w/w) containing various amounts of CN (v/v)] were sandwiched between the transparent ITO anode and cathode. The devices were prepared following the same procedure described for the fabrication of the BHJ devices, except that, for the hole-only devices, Ca was replaced with MoO_3 [work function (Φ) = 5.3 eV] and, for the electron-only devices, the PEDOT:PSS layer was replaced with Cs_2CO_3 [work function (Φ) = 2.9 eV]. In the hole-only devices, MoO_3 was thermally evaporated to a thickness of 20 nm and then capped with 50 nm of Al on top of the active layer. In the electron-only devices, Cs_2CO_3 was thermally evaporated to a thickness of approximately 2 nm on top of the transparent ITO. For both devices, annealing of the active layer was performed at 130 °C for 20 min. The SCLC method was used to evaluate the hole and electron mobilities of the small-molecule blend films of BT6OT:$PC_{71}BM$, at a weight ratio of 1 : 0.75 after the addition of various amounts of CN (0.25, 0.50, or 1 vol%), in hole- and electron-only devices. The electron and hole mobilities were determined by fitting the plots of the dark current–voltage (J–V) curves for single-carrier devices to the SCLC model. The dark current was given by

$$J = 9\varepsilon_0\varepsilon_r\mu V^2/8L^3$$

where $\varepsilon_0\varepsilon_r$ is the permittivity of the polymer, μ is the carrier mobility, and L is the device thickness.

Results and discussion

Synthesis and structural characterization

Scheme 1 presents the synthetic routes toward compounds BT4OT and BT6OT. The syntheses of some of the compounds, performed with slight modifications of reported procedures, are described in the ESI.†[14,23,25] Friedel–Crafts acylation of 2,3-dibromothiophene gave ketone **1**; Suzuki–Miyaura cross-coupling of **1** with thiophene-3-boronic acid led to assembly of trithiophene system **2**, which underwent subsequent oxidative ring closure with DDQ to form BT core **3**. The acyl-functionalized BT **3** was then converted using the Huang Minlon modification to the alkyl-BT **4**. Compound **4** was converted to **5** through deprotonation with *n*-BuLi followed by addition of trimethyltin chloride. Compounds **10** and **11** were synthesized through Knoevenagel condensations of **7** and **9**, respectively, which were then symmetrically Stille coupled with **5** to obtain BT4OT and BT6OT, respectively. Both BT4OT and BT6OT are

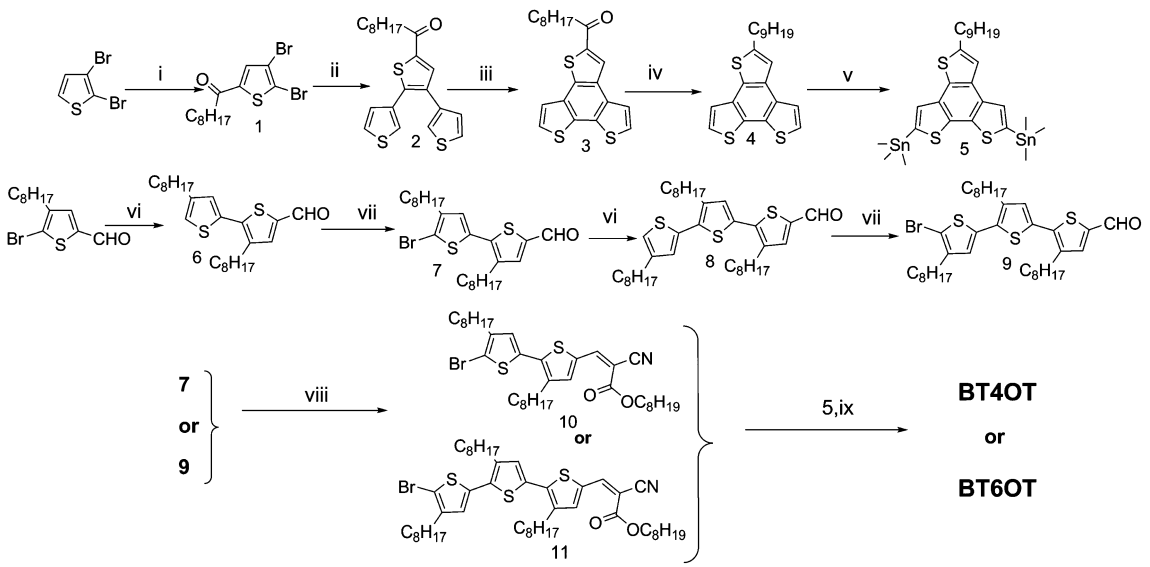

Scheme 1 Synthesis of BT4OT and BT6OT. *Reagents and conditions*: (i) anhydrous $AlCl_3$, $C_8H_{17}COCl$, 0 °C; (ii) toluene, 3-thiopheneboronic acid, Na_2CO_3, 90 °C, $Pd(PPh_3)_4$, 24 h; (iii) DDQ, BF_3OEt_2, CH_2Cl_2, 0 °C to RT, Zn, MeOH; (iv) $NH_2NH_2{\cdot}H_2O$, KOH, ethylene glycol; (v) THF, −78 °C, $SnMe_3Cl$; (vi) trimethyl(4-octylthien-2-yl)-stannane, $Pd(PPh_3)_4$, toluene, reflux; (vii) NBS, $CHCl_3$–AcOH (1 : 1), 0 °C then RT overnight; (viii) $CHCl_3$, octylcyanoacetate, RT; (ix) $Pd(PPh_3)_4$, toluene, reflux.

Published on 07 May 2013. Downloaded by National Chiao Tung University on 28/04/2014 01:59:56.

soluble in common organic solvents, including CH_2Cl_2, $CHCl_3$, THF, chlorobenzene (CB), and dichlorobenzene.

Optical properties

We investigated the photophysical characteristics of BT4OT and BT6OT by recording their UV-Vis absorption spectra from $CHCl_3$ solutions as well as solid films on glass substrates (Fig. 2); Table 1 lists the normalized absorption maxima and optical band gaps (E_g^{opt}) for both the solutions and solid films. In solution, BT4OT experienced two distinct absorptions with maximum wavelengths of 373 and 483 nm, respectively. The former is due to π–π* transitions and the latter due to intramolecular charge transfer (ICT) between the donor benzotrithiophene (BT) moiety and the acceptor cyanoacetate moieties.[23,25] For BT6OT, in contrast, overlap of the π–π* transition and ICT bands led to the appearance of a new broad band at 466 nm covering more of the visible region.[19,22] The attachment of two lateral alkyl thiophene units resulted in an 18 nm blue shift in the absorptions of BT6OT in solution, relative to BT4OT, presumably because of increased disorder in the conjugated system, due to steric effects of the alkyl side chains.[26,27] For their solid films, the absorption maxima of BT4OT and BT6OT appeared at 569 and 561 nm, red-shifted by approximately 86 and 96 nm, respectively, relative to those in solution, attributable to the highly coplanar structures of the BT units and corresponding strong π–π interchain interactions.[17–20,28] The optical band gaps calculated from the onsets of absorptions of BT4OT and BT6OT in the solid state were 1.75 and 1.72 eV, respectively; these almost-identical values presumably resulted from the similar electron-withdrawing abilities of the two terminal cyanoacetate moieties.

Electrochemical properties

We used cyclic voltammetry (CV) to investigate the redox behavior of BT4OT and BT6OT and their electronic states (*i.e.*, HOMO/LUMO levels). Fig. 3 displays the oxidation and reduction cyclic voltammograms of BT4OT and BT6OT; Table 1 summarizes the electrochemical properties of BT4OT and BT6OT, including their onset potentials for oxidation (E_{ox}^{onset}) and reduction (E_{red}^{onset}) and their electrochemical band gaps. BT4OT and BT6OT both underwent oxidation (p-doping), due to their electron-rich BT units, in the positive potential range and reduction (n-doping), and due to their electron-poor cyanoacetate units, in the negative potential range.[27] The values of E_{ox}^{onset} and E_{red}^{onset} were +1.11 and −0.74 V, respectively, for BT4OT and +1.06 and −0.78 V, respectively, for BT6OT. We estimated the HOMO and LUMO energy levels from the oxidation and

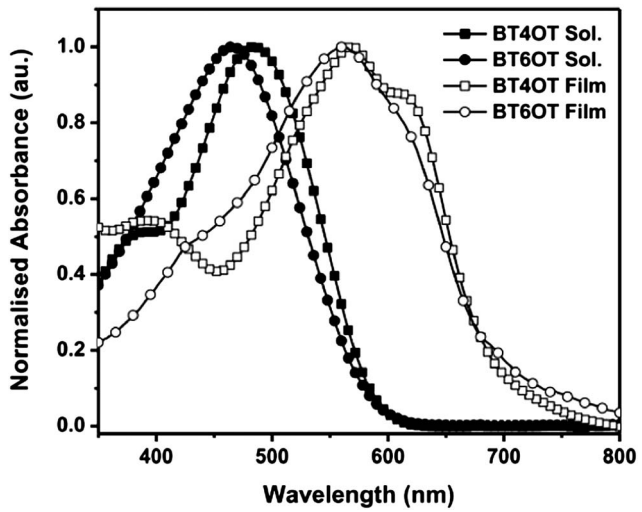

Fig. 2 Normalized UV-Vis absorption spectra of BT4OT and BT6OT as dilute solutions in $CHCl_3$ and as thin films on glass surfaces at room temperature.

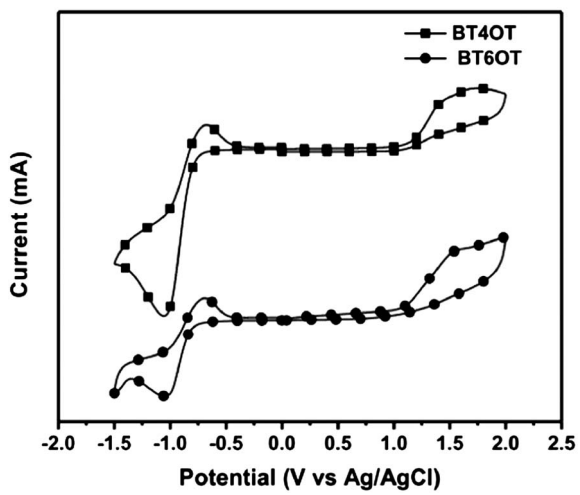

Fig. 3 Cyclic voltammograms of BT4OT and BT6OT as thin films (scan rate: 100 mV s^{-1}).

Table 1 Optical and electrochemical properties of BT4OT and BT6OT

	Solution[a]	Solid film[b]	Energy levels		Band gaps[d]	
Small molecule	$\lambda_{max,abs}$ (nm)	$\lambda_{max,abs}$ (nm)	E_{onset}^{ox} (V)/HOMO[c] (eV)	E_{onset}^{red} (V)/LUMO[c] (eV)	E_g^{ec} (eV)	E_g^{opt} (eV)
TT4OT	380, 483	396, 569, 618	1.11/−5.48	−0.74/−3.61	1.85	1.75
TT6OT	465	561	1.06/−5.41	−0.78/−3.57	1.84	1.72

[a] Dilute solution in $CHCl_3$. [b] Spin-coated from $CHCl_3$ solution onto the glass surface. [c] $E_{HOMO}/E_{LUMO} = [-(E_{onset} - E_{onset(FC/FC^+ vs. Ag/Ag^+)}) - 4.8]$ eV, where 4.8 eV is the energy level of ferrocene below the vacuum level and $E_{onset(FC/FC^+ vs. Ag/Ag^+)} = 0.45$ eV. [d] Electrochemical band gap: $E_g^{ec} = E_{ox/onset} - E_{red/onset}$; optical band gap: $E_g^{opt} = 1240/\lambda_{edge}$.

 This journal is © The Royal Society of Chemistry 2013

Published on 07 May 2013. Downloaded by National Chiao Tung University on 28/04/2014 01:59:56.

reduction potentials and the reference energy level for ferrocene (4.8 eV below the vacuum level) according to the equations[15,29]

$$E_{\mathrm{HOMO/LUMO}} = [-(E_{\mathrm{onset}} - E_{\mathrm{onset(FC/FC^{+}\ vs.\ Ag/Ag^{+})}}) - 4.8]\ \mathrm{eV}$$

and

$$\text{band gap} = E^{\mathrm{ox}}_{\mathrm{onset}} - E^{\mathrm{red}}_{\mathrm{onset}} \quad (1)$$

where $E_{\mathrm{onset(FC/FC^{+}\ vs.\ Ag/Ag^{+})}}$ was equal to 0.45 eV. The calculated HOMO and LUMO energy levels were −5.48 and −3.61 eV, respectively, for BT4OT and −5.41 and −3.57 eV, respectively, for BT6OT. The HOMO and LUMO of BT6OT were slightly higher in energy than those of BT4OT, presumably because of the former featured additional electron-rich alkyl thiophene rings surrounding the BT moieties.[30] Enhancing the electron-donating ability on both sides of the BT core decreased the oxidation potential and decreased the electron-withdrawing ability in BT6OT.[29,31] The electrochemical band gaps, calculated from the oxidation and reduction potentials, were approximately 1.85 eV for BT4OT and 1.84 eV for BT6OT.

The low HOMO energy levels of BT4OT and BT6OT suggested that we might obtain solar cell devices exhibiting high open-circuit voltages, because the value of V_{oc} is directly proportional to the difference between the HOMO energy level of the donor and the LUMO energy level of the acceptor (PCBM).[29,30] For the exciton binding energy of BT4OT and BT6OT to be overcome to result in efficient electron transfer from the donor to the acceptor, we required the LUMO energy level of the electron donor (BT4OT or BT6OT) to be positioned above the LUMO energy level of the acceptor by at least 0.3 eV.[29] The electrochemical band gaps were in good agreement with the optical band gaps; in addition, they were also in a desirable range for use in organic photovoltaic applications.

Photovoltaic properties

Our motivation for designing BT-based small molecules was to investigate their potential applications in bulk heterojunction (BHJ) solar cells; here, we used BT4OT and BT6OT as electron donors and $PC_{61}BM$ or $PC_{71}BM$ as electron acceptors in devices having the configuration ITO/PEDOT:PSS/small molecule:PCBM/Ca/Al. Details of the performance of the BHJ devices incorporating BT4OT and BT6OT are presented in the ESI.† To achieve better performance in photovoltaic devices, $CHCl_3$ was chosen as the solvent to obtain active layers of the blended small molecules with good film qualities. Table 2 reveals that the best performance for the photovoltaic device based on BT4OT blended with $PC_{61}BM$ at a weight ratio of 1 : 0.75 (w/w) in $CHCl_3$ was a PCE of 2.98% ($V_{\mathrm{oc}} = 0.88$ V; $J_{\mathrm{sc}} = 6.32$ mA cm^{-2}; FF = 53.6); for the device based on BT6OT, it was a PCE of 3.19% ($V_{\mathrm{oc}} = 0.86$ V; $J_{\mathrm{sc}} = 6.78$ mA cm^{-2}; FF = 54.8%) (see Fig. S6 and S7, ESI†). The values of V_{oc} we obtained for both the BT4OT- and BT6OT-based devices are higher than those reported previously for all other BT-based PCS devices.[21–23] The presence of two additional octylthiophene units in the main chain of BT6OT is the reason for its enhanced value of J_{sc} relative to that of BT4OT. We optimized the BT6OT-based device by blending BT6OT with different ratios of $PC_{71}BM$; Fig. 4 and Table 2 summarize the results. The highest PCE (3.61%; $V_{\mathrm{oc}} = 0.88$ V; $J_{\mathrm{sc}} = 7.39$ mA cm^{-2}; FF = 56.9%) was that recorded for the device we prepared from BT6OT blended with $PC_{71}BM$ at a ratio of 1 : 0.75 (w/w).

An additive solvent having a boiling point higher than that of the parent solvent and exhibiting selective solubility for the donor and the acceptor can deeply impact the semiconducting properties of an organic material.[10,13,32] We further optimized the device incorporating BT6OT through the addition of various volumes of CN in the active layer to control the nanoscale morphology by minimizing molecular phase aggregation (Fig. 5). Adding 0.25 vol% of CN to the BT6OT:$PC_{71}BM$ film

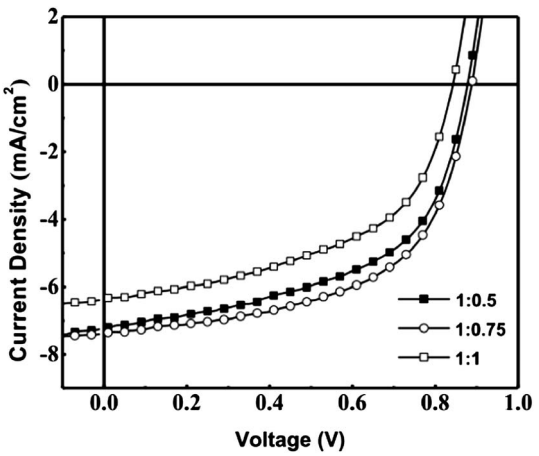

Fig. 4 *J–V* curves of BHJ solar cell devices incorporating BT6OT:$PC_{71}BM$ blends of various weight ratios, recorded under AM 1.5G irradiation at 100 mW cm^{-2}.

Table 2 Photovoltaic properties and electron and hole mobilities of BT4OT and BT6OT

Active layer blend	Blend ratio	Additive (vol%)	V_{oc} (V)	J_{sc} (mA cm^{-2})	FF %	PCE	Hole mobility (μ_{h}, cm^2 V^{-1} s^{-1})	Electron mobility (μ_{e}, cm^2 V^{-1} s^{-1})	$\mu_{\mathrm{e}}/\mu_{\mathrm{h}}$
BT4OT:$PC_{61}BM$	1 : 0.75	—	0.88	6.32	53.6	2.98	—	—	—
BT6OT:$PC_{61}BM$	1 : 0.75	—	0.86	6.78	54.8	3.19	—	—	—
BT6OT:$PC_{71}BM$	1 : 0.50	—	0.88	7.23	54.1	3.44	2.53×10^{-4}	3.71×10^{-4}	1.46
BT6OT:$PC_{71}BM$	1 : 0.75	—	0.88	7.39	56.9	3.61	2.89×10^{-4}	3.86×10^{-4}	1.33
BT6OT:$PC_{71}BM$	1 : 1	—	0.85	6.35	50.7	2.74	2.47×10^{-4}	6.51×10^{-4}	2.63
BT6OT:$PC_{71}BM$	1 : 0.75	0.25	0.86	9.94	59.1	5.05	6.61×10^{-4}	15.11×10^{-4}	2.28
BT6OT:$PC_{71}BM$	1 : 0.75	0.50	0.85	7.58	54.6	3.52	4.89×10^{-4}	10.03×10^{-4}	2.05
BT6OT:$PC_{71}BM$	1 : 0.75	0.75	0.76	0.829	30.4	0.23	2.37×10^{-4}	6.28×10^{-4}	2.64

Published on 07 May 2013. Downloaded by National Chiao Tung University on 28/04/2014 01:59:56.

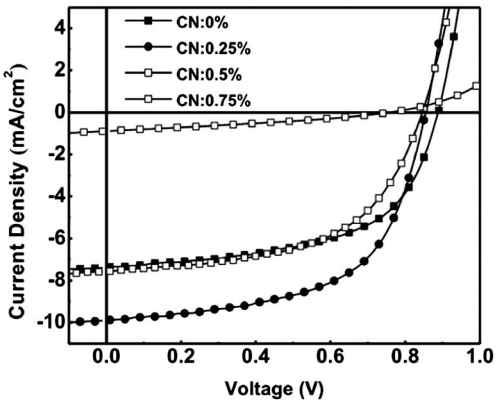

Fig. 5 *J–V* characteristics of solar cells incorporating BT6OT:$PC_{71}BM$ (1 : 0.75) and various amounts (vol%) of CN, recorded under AM 1.5G irradiation at 100 mW cm^{-2}.

resulted in remarkable enhancements in the value of J_{sc} (from 7.39 to 9.94 mA cm^{-2}) and the FF, while maintaining a constant value of V_{oc}, leading to the PCE increase from 3.65 to 5.05%. We suspect that the addition of the solvent additive improved the value of J_{sc} through the generation of a greater number of photocharge carriers and improved transport through the formation of a favorable film morphology.[32] Nevertheless, addition of higher fractions of CN (*e.g.*, 0.50 or 0.75 vol%) in the BT6OT:$PC_{71}BM$ blend film decreased the PCEs and the photovoltaic parameters dramatically (Table 2); this behavior presumably resulted from morphological disorder, as evidenced using atomic force microscopy (AFM).[13,32]

The surface morphology of the active layer in a solar cell device is also a key parameter affecting its performance.[17,18,33] Fig. 6 displays AFM and phase images of the morphologies of the BT6OT:$PC_{71}BM$ (1 : 0.75) blend films cast without CN and with the optimized concentration of CN. The AFM image of

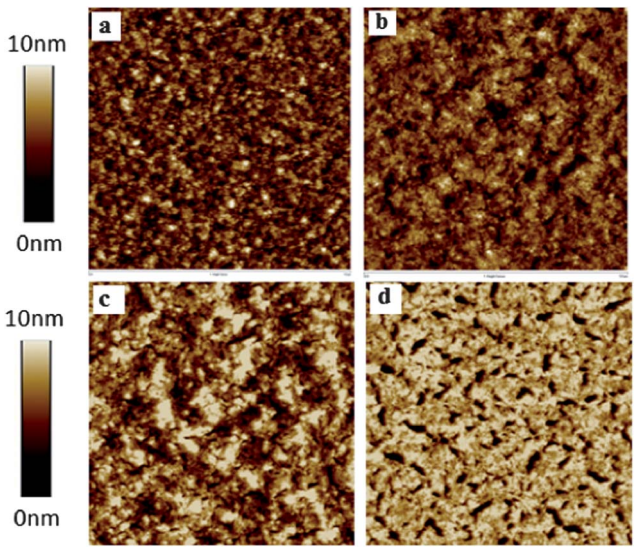

Fig. 6 AFM images of BT6OT:$PC_{71}BM$ (1 : 0.75) blends containing various amounts of CN as a processing additive: (a) 0, (b) 0.25, (c) 0.50, and (d) 1 vol%.

BT6OT:$PC_{71}BM$ (1 : 0.75) reveals a smooth surface with little aggregation between BT6OT and $PC_{71}BM$, with a root-mean-square roughness (R_{rms}) of 1.64 nm. Even fewer aggregated domains, resulting in a value of R_{rms} of 1.54 nm, appeared in the film after addition of 0.25 vol% of CN to BT6OT:$PC_{71}BM$ (1 : 0.75), leading to a dramatic enhancement in PCE from 3.651 to 5.05%.[14] The PCEs decreased dramatically, however, to 3.52 and 0.23% after the addition of 0.50 and 0.75 vol%, respectively, of CN to the BT6OT:$PC_{71}BM$ (1 : 0.75) blend, leading to poorer morphologies with highly aggregated domains and values of R_{rms} of 1.95 and 2.08 nm, respectively. These lower values of R_{rms} increased the diffusional escape probabilities for the mobile charge carriers, thereby minimizing their recombination.[15] It has been noted previously from AFM images that lower degrees of aggregation of BT6OT and PCBM inhibit charge recombination, while enhanced π–π stacking improves the transport of photogenerated charges, leading to higher values of J_{sc}.[15,27,29]

Hole and electron mobilities are key parameters for both material design and device fabrication.[15] Fig. S8 (ESI†) presents *J–V* curves of the hole and electron mobilities (μ_e and μ_h, respectively) of the optimized blend BT6OT:$PC_{71}BM$ (1 : 0.75) in the absence of CN and in the presence of the optimal CN concentration, as measured using the space-charge limited current (SCLC) model. Hole and electron mobilities of the device containing BT6OT:$PC_{71}BM$ (1 : 0.75) were 2.89×10^{-4} and 3.86×10^{-4} cm^2 V^{-1} s^{-1}, respectively, providing a μ_e/μ_h ratio of 1.33 (Table 2). A dramatic increase of μ_e (~3.9 fold) and μ_h (~2.4 fold) was observed after we had added 0.25 vol% of the processing additive active layer BT6OT:$PC_{71}BM$ (1 : 0.75) blend. Less-balanced charge transport ratios (μ_e/μ_h = 2.47 and 2.64, see Table 2), with dramatically decreased values of J_{sc}, resulted when we prepared devices of higher CN contents (0.5 and 0.75 vol%, respectively) compared to 0.25 vol% of CN μ_e/μ_h = 2.05. The highest hole mobility of the optimized device with added CN (0.25 vol%) was 6.61×10^{-4} cm^2 V^{-1} s^{-1}, which is an explanation of the highest value of J_{sc} (9.97 mA cm^{-2}) for this device among all of those we tested (containing 0, 0.50, or 0.75 vol% of CN).[15,27]

Next, we recorded external quantum efficiency (EQE) plots for the devices containing BT6OT:$PC_{71}BM$ (1 : 0.75) films, prepared in the absence of CN and in the presence of the optimal amount of CN, under monochromatic light. Fig. 7 reveals that all of the devices exhibited good EQE behavior, with a broad photoresponsive range extending from 350 to 700 nm. The solar cell device containing BT6OT:$PC_{71}BM$ (1 : 0.75, w/w) with 0.25 vol% of CN provided the highest EQE (*ca.* 47%) among all the tested devices.[15,20] The devices containing BT6OT:$PC_{71}BM$ (1 : 0.75, w/w) with 0 and 0.5 vol% of CN displayed similar EQEs (*ca.* 41%), values of J_{sc} (7.39 and 7.58 mA cm^{-2}, respectively) and PCEs (3.61 and 3.52%, respectively). A dramatic decrease, however, in the photocurrent of the device containing BT6OT:$PC_{71}BM$ (1 : 0.75, w/w) with 0.75 vol% of CN resulted in the lowest values of J_{sc} and PCE, due to a low EQE of approximately 5%. We attribute this poor device performance to a serious degree of material aggregation associated with the decrease in the area of the heterojunction interface. Thus, in

 This journal is © The Royal Society of Chemistry 2013

Published on 07 May 2013. Downloaded by National Chiao Tung University on 28/04/2014 01:59:56.

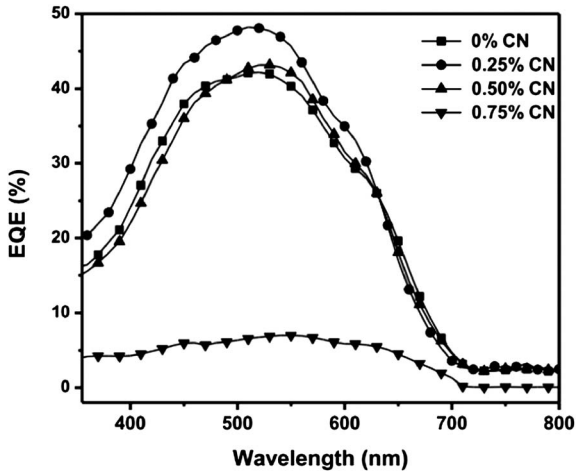

Fig. 7 EQE curves of BHJ solar cells incorporating BT6OT:$PC_{71}BM$ blends containing various amounts of CN as a processing additive.

this study, the device containing BT6OT:$PC_{71}BM$ (1 : 0.75, w/w) with 0.25 vol% of CN exhibited the highest values of J_{sc} (9.94 mA cm^{-2}) and PCE (5.05%), due to its greatest EQE response and superior charge transport properties and nanoscale morphology relative to all of the other tested devices.

Conclusions

We have developed a symmetrical synthetic approach toward the novel, planar BT-based A–D–A small molecules, BT4OT and BT6OT, for use in solution-processed BHJ solar cells. The number of octylthiophene units significantly affected the optical, electrochemical, and photovoltaic properties of BT4OT and BT6OT. A photovoltaic device containing a blend of BT6OT:$PC_{71}BM$ at a weight ratio of 1 : 0.75 provided the highest PCE (5.05%), with a high value of V_{oc} (0.88 V) and a notable FF (59.1%), after we had added 0.25 vol% of CN as a processing additive to the blend film. Devices incorporating BT4OT and BT6OT exhibited values of V_{oc} higher than those of devices featuring all other previously reported BT-containing polymer counterparts. These outstanding results suggest that small molecules might soon provide device performances comparable with those of their polymeric counterparts.

Acknowledgements

We thank the National Science Council of Taiwan (NSC 100-2120-M-009-004 and 101-2221-E-001-010), the Academia Sinica Research Project on Nano Science and Technology, and the Thematic Project of Academia Sinica, Taiwan (AS-100-TP-A05) for financial support.

References

1 A. J. Heeger, *Chem. Soc. Rev.*, 2010, **39**, 2354.
2 A. C. Arias, J. D. MacKenzie, I. McCulloch, J. Rivnay and A. Salleo, *Chem. Rev.*, 2010, **110**, 3.
3 Y. J. Cheng, S. H. Yang and C. S. Hsu, *Chem. Rev.*, 2009, **109**, 5868.
4 X. Zhao and X. Zhan, *Chem. Soc. Rev.*, 2011, **40**, 3728.
5 Z. He, C. Zhong, X. Huang, W.-Y. Wong, H. Wu, L. Chen, S. Su and Y. Cao, *Adv. Mater.*, 2011, **23**, 4636.
6 L. Dou, J. Gao, E. Richard, J. You, C. C. Chen, K. C. Cha, Y. He, G. Li and Y. Yang, *J. Am. Chem. Soc.*, 2012, **134**, 10071.
7 Y. Sun, G. C. Welch, W. L. Leong, C. J. Takacs, G. C. Bazan and A. J. Heeger, *Nat. Mater.*, 2012, **11**, 44.
8 S. Loser, C. J. Bruns, H. Miyauchi, R. P. Ortiz, A. Facchetti, S. I. Stupp and T. J. Marks, *J. Am. Chem. Soc.*, 2011, **133**, 8142.
9 J. Zhang, D. Deng, C. He, Y. J. He, M. J. Zhang, Z. G. Zhang, Z. J. Zhang and Y. F. Li, *Chem. Mater.*, 2011, **23**, 817.
10 A. Mishra and P. Bäuerle, *Angew. Chem., Int. Ed.*, 2012, **51**, 2020.
11 Y. Lin, Y. Li and X. Zhan, *Chem. Soc. Rev.*, 2012, **41**, 4245.
12 Y. Li, Q. Guo, Z. Li, J. Pei and W. Tian, *Energy Environ. Sci.*, 2010, **3**, 1427.
13 T. S Poll, J. A. Love, T.-Q. Nguyen and G. C. Bazan, *Adv. Mater.*, 2012, **24**, 3646.
14 Y. Liu, X. Wan, F. Wang, J. Zhou, G. Long, J. Tian and Y. Chen, *Adv. Mater.*, 2011, **23**, 5387.
15 D. Sahu, C. H. Tsai, H. Y. Wei, K. C. Ho, F. C. Chang and C. W. Chu, *J. Mater. Chem.*, 2012, **22**, 7945.
16 M. Chen, W. Fu, M. Shi, X. Hu, J. Pan, J. Ling, H. Li and H. Chen, *J. Mater. Chem. A*, 2013, **1**, 105.
17 Z. Li, G. He, X. Wan, Y. Liu, J. Zhou, G. Long, Y. Zuo, M. Zhang and Y. Chen, *Adv. Energy Mater.*, 2012, **2**, 74.
18 Y. Liu, X. Wan, F. Wang, J. Zhou, G. Long, J. Tian, J. You, Y. Yang and Y. Chen, *Adv. Energy Mater.*, 2011, **1**, 771.
19 J. Zhou, X. Wan, Y. Liu, G. Long, F. Wang, Z. Li, Y. Zuo, C. Li and Y. Chen, *Chem. Mater.*, 2011, **23**, 4666.
20 J. Zhou, X. Wan, Y. Liu, Y. Zuo, G. He, G. Long, W. Ni, C. Li, X. Su and Y. Chen, *J. Am. Chem. Soc.*, 2012, **134**, 16345.
21 C. B. Nielsen, B. C. Schroeder, A. Hadipour, B. P. Rand, S. E. Watkins and I. McCulloch, *J. Mater. Chem.*, 2011, **20**, 17642.
22 C. B. Nielsen, R. S. Ashraf, B. C. Schroeder, P. D'Angelo, S. E. Watkins, K. Song, T. D. Anthopoulos and I. McCulloch, *Chem. Commun.*, 2012, **48**, 5832.
23 S. C. Lan, P. A. Yang, M. J. Zhu, C. M. Yu, J. M. Jiang and K. H. Wei, *Polym. Chem.*, 2013, **4**, 1132.
24 B. C. Schroeder, C. B. Nielsen, Y. J. Kim, J. Smith, Z. Huang, J. Durrant, S. E. Watkins, K. Song, T. D. Anthopoulos and I. McCulloch, *Chem. Mater.*, 2011, **23**, 4025.
25 C. B. Nielsen, J. M. Fraser, B. C. Schroeder, J. Du, A. J. White, W. Zhang and I. McCulloch, *Org. Lett.*, 2011, **13**, 2414.
26 H. C. Chu, D. Sahu, Y. C. Hsu, H. Padhy, D. Patra, J. T. Lin, D. Bhattacharya, K. L. Lu, K. H. Wei and H. C. Lin, *Dyes Pigm.*, 2012, **93**, 1488.
27 D. Patra, D. Sahu, H. Padhy, D. Kekuda, C. W. Chu, K. H. Wei and H. C. Lin, *Macromol. Chem. Phys.*, 2011, **212**, 1960.
28 A. Tang, L. Li, Z. Lu, J. Huang, H. Jia, C. Zhan, Z. Tan, Y. Li and J. Yao, *J. Mater. Chem. A*, 2013, **1**, 5747.
29 D. Patra, M. Ramesh, D. Sahu, H. Padhy, C. W. Chu, K. H. Wei and H. C. Lin, *J. Polym. Sci., Part A: Polym. Chem.*, 2012, **50**, 967.

30 I. H. Jung, J. Yu, E. Jeong, S. Kwon, H. Kong, K. Lee, H. Y. Woo and H. K. Shim, *Chem.–Eur. J.*, 2010, **16**, 3743.
31 D. Patra, M. Ramesh, D. Sahu, H. Padhy, C. W. Chu, K. H. Wei and H. C. Lin, *Polymer*, 2012, **53**, 1219.
32 J. K. Park, C. Kim, B. Walker, T. Q. Nguyen and J. H. Seo, *RSC Adv.*, 2012, **2**, 2232.
33 Y. Lin, Z.-G. Zhang, Y. Li, D. Zhu and X. Zhan, *J. Mater. Chem. A*, 2013, **1**, 5128.

Published on 07 May 2013. Downloaded by National Chiao Tung University on 28/04/2014 01:59:56.

This journal is © The Royal Society of Chemistry 2013